# Solitons and lumps in the cylindrical Kadomtsev–Petviashvili equation. II. Lumps and their interactions

Cite as: Chaos 34, 013132 (2024); doi: 10.1063/5.0175716
Submitted: 8 September 2023 · Accepted: 24 December 2023 ·
Published Online: 22 January 2024



Zhao Zhang,[1] Wencheng Hu,[2] Qi Guo,[1,a)] and Yury Stepanyants[3,4,a)]

## AFFILIATIONS

[1]Guangdong Provincial Key Laboratory of Nanophotonic Functional Materials and Devices, South China Normal University, Guangzhou 510631, People's Republic of China
[2]School of Physics and Optoelectronic Engineering, Zhongyuan University of Technology, Zhengzhou 450007, China
[3]School of Mathematics, Physics and Computer Sciences, University of Southern Queensland, Toowoomba, QLD 4350, Australia
[4]Department of Applied Mathematics,
Nizhny Novgorod State Technical University, n.a. R.E. Alekseev, 24 Minin St., Nizhny Novgorod 603950, Russia

[a)]**Authors to whom correspondence should be addressed: Email address:** guoq@scnu.edu.cn and Yury.Stepanyants@usq.edu.au

## ABSTRACT

We study solitary waves in the cylindrical Kadomtsev–Petviashvili equation designated to media with positive dispersion (the cKP1 equation). By means of the Darboux–Matveev transform, we derive exact solutions that describe two-dimensional solitary waves (lumps), lump chains, and their interactions. One of the obtained solutions describes the modulation instability of outgoing ring solitons and their disintegration onto a number of lumps. We also derive solutions describing decaying lumps and lump chains of a complex spatial structure—ripplons. Then, we study normal and anomalous (resonant) interactions of lump chains with each other and with ring solitons. Results obtained agree with the numerical data presented in Part I of this study [Hu *et al.*, Chaos (2024)].





**This paper represents Part II of our study on exact solutions of the cKP1 equation designated to waves in media with positive dispersion. In Part I, we have studied primarily axisymmetrical solutions in the form of specific cylindrical solitons. It has been shown that such solutions are unstable with respect to the modulation of their fronts on the azimuthal direction in positive dispersion media. Here, we revise the earlier obtained exact solutions to the cKP1 equation and show that formally correct solutions that are not periodic on the azimuthal variable are not physically acceptable. By means of the Darboux–Matveev transform, we derive various exact solutions that describe, in particular, the nonlinear stage of the modulation instability of expanding ring solitons and formation of two-dimensional solitons—lumps. Other derived solutions describe normal and anomalous (resonance) interactions of lump chains with each other and with ring solitons. Solutions obtained can be of interest in application to physical processes occurring in plasma and other media with positive dispersion.**

## I. INTRODUCTION

In Part I of this study,[1] we considered soliton-type and self-similar solutions of the cylindrical Kadomtsev–Petviashvili (cKP) equation known also as the Johnson equation,[2]

$$\frac{\partial}{\partial t}\left(\frac{\partial u}{\partial r}+\frac{1}{c}\frac{\partial u}{\partial t}-\frac{\alpha}{c}u\frac{\partial u}{\partial t}-\frac{\beta}{2c^5}\frac{\partial^3 u}{\partial t^3}+\frac{u}{2r}\right)=\frac{c}{2r^2}\frac{\partial^2 u}{\partial \varphi^2}, \quad (1.1)$$

where $u(t,r,\varphi)$ is wave perturbation, which depends on time $t$ and two spatial coordinates in the cylindrical frame $(r,\varphi)$, $c$ is the speed of long linear waves, and $\alpha$ and $\beta$ are the coefficient of nonlinearity and dispersion, respectively, which depend on parameters of a particular physical problem. Equation (1.1) is presented here in dimensional physical variables. In its derivation, it was assumed that the effects of non-linearity, dispersion, geometrical spreading, and variations along the azimuthal direction are small and of the same order of smallness. Therefore, this equation and its solutions are not

valid near the center of the polar coordinate frame where the distance $r$ is less or comparable with the characteristic width of a wave perturbation $\Lambda$. To derive solutions to the cKP equation, it is necessary to reduce it to the dimensionless "standard" form, which is traditionally used in many publications (see, for example, Ref. 3),

$$\frac{\partial}{\partial\tau}\left(\frac{\partial U}{\partial r}+6U\frac{\partial U}{\partial\tau}+\frac{\partial^3 U}{\partial\tau^3}+\frac{U}{2r}\right)=-\sigma^2\frac{3}{r^2}\frac{\partial^2 U}{\partial\theta^2}, \tag{1.2}$$

$$\text{where}\quad r=r,\ \tau=c^2\left(\frac{2}{\beta c}\right)^{1/3}\left(\frac{r}{c}-t\right),\quad \theta=\varphi\sqrt{6c\sigma^2\left(\frac{2}{\beta c}\right)^{1/3}}, \tag{1.3}$$

$$U=\frac{\alpha u c}{6}\left(\frac{2}{\beta c}\right)^{1/3}.$$

Here, the parameter $\sigma^2=\pm1$ determines the type of the cKP equation; its sign is the same as the sign of the dispersion parameter $\beta$; therefore, $\beta\sigma^2>0$. The case with $\sigma^2=1$ pertains to the cKP2 equation that describes waves in media with negative dispersion (for example, surface or internal waves in shallow water), whereas $\sigma^2=-1$ pertains to the cKP1 equation applicable to waves in media with positive dispersion (for example, waves in a magnetized plasma). Such a classification based on the parameter $\sigma^2$ is very similar to the classification of the conventional quasi-one-dimensional KP equation (see, for example, Refs. 4 and 5).

If function $U$ does not depend on $\theta$, then Eq. (1.2) reduces to the cylindrical Korteweg–de Vries (cKdV) equation. Exact and approximate solutions as well as numerical solutions of the cKdV equation in the form of pulse-type outgoing waves ("cylindrical solitons") were presented in Part I of this study.[1] It was shown also that axis-symmetric ring solitons are unstable with respect to azimuthal perturbations in positive dispersive media with $\beta<0$ ($\sigma^2=-1$). A numerical experiment has demonstrated that the development of modulation of ring solitons leads to the emergence of compact two-dimensional patterns, which can be treated as chains of lumps.[1] This process is similar to the development of modulation instability of plane waves in positive dispersive media.[6] In this paper, we continue studying by analytical methods the emergence of lump chains from the modulated ring solitons, as well as normal and anomalous interactions of lump chains.

## II. THE DARBOUX–MATVEEV TRANSFORM

In this section, we present various exact solutions to the cKP1 equation through the Darboux–Matveev transform (DMT) method. First, we briefly outline the DMT for the cKP1 equation following Refs. 3 and 7, and then, we will use the method to construct new solutions.

Let us consider the cKP1 equation in the "standard form" (1.2) with $\sigma=i$. As well-known, this equation is exactly solvable through the inverse scattering transform;[8,9] it can be presented as the compatibility condition of the linear set of equations,[3,7,8]

$$\begin{aligned} i\frac{\partial\psi}{\partial\theta}&=r\frac{\partial^2\psi}{\partial\tau^2}+\left(rU-\frac{\tau}{12}\right)\psi,\\ \frac{\partial\psi}{\partial r}&=-4\frac{\partial^3\psi}{\partial\tau^3}-6U\frac{\partial\psi}{\partial\tau}-3\left(\frac{\partial U}{\partial\tau}+\frac{iV}{r}\right)\psi, \end{aligned} \tag{2.1}$$

where $\partial V/\partial\tau=\partial U/\partial\theta$. The adjoint set of equations is

$$\begin{aligned} -i\frac{\partial\chi}{\partial\theta}&=r\frac{\partial^2\chi}{\partial\tau^2}+\left(rU-\frac{\tau}{12}\right)\chi,\\ \frac{\partial\chi}{\partial r}&=-4\frac{\partial^3\chi}{\partial\tau^3}-6U\frac{\partial\chi}{\partial\tau}-3\left(\frac{\partial U}{\partial\tau}-\frac{iV}{r}\right)\chi. \end{aligned} \tag{2.2}$$

Here, function $\chi(r,\theta,\tau,\lambda)$ is complex-conjugate of function $\psi(r,\theta,\tau,\lambda)$, i.e., $\chi=\psi^*$, where $\lambda$ is a complex parameter. As shown by Klein *et al.*,[3] a solution to the cKP1 equation via the $N$-fold DMT (short for Darboux–Matveev transform) with the seed solution $U=0$ can be expressed through the Hirota transform,

$$U=2\frac{\partial^2}{\partial\tau^2}\ln\Gamma, \tag{2.3}$$

with

$$\Gamma=\begin{vmatrix} p_1+\langle\psi_1,\chi_1\rangle & \langle\psi_1,\chi_2\rangle & \cdots & \cdots & \langle\psi_1,\chi_N\rangle\\ \langle\psi_2,\chi_1\rangle & p_2+\langle\psi_2,\chi_2\rangle & & & \langle\psi_2,\chi_N\rangle\\ \vdots & & \ddots & & \vdots\\ \vdots & & & \ddots & \vdots\\ \langle\psi_N,\chi_1\rangle & \langle\psi_N,\chi_2\rangle & \cdots & \cdots & p_N+\langle\psi_N,\chi_N\rangle \end{vmatrix}. \tag{2.4}$$

Here, $p_l$, $l=1,2,\ldots,N$ are real parameters, and the symbols $\langle\psi_l,\chi_j\rangle$ stand for the integral,

$$\langle\psi_l,\chi_j\rangle=\int\psi(\tau,\theta,r,\lambda_l)\,\chi(\tau',\theta,r,\lambda_j)\,d\tau. \tag{2.5}$$

In order to obtain a smooth analytical solution, the integration path of Eq. (2.5) can be specifically determined based on the specific type of the integrated function. Morever, $\psi_l$, $\chi_l$ are the solutions of the Lax pair [Eqs. (2.1) and (2.2)] corresponding to the zero seed solution with the specific spectral parameter $\lambda_l$.

If we choose a particular solution to Eqs. (2.1)–(2.2) with $U=0$ in an exponential form, then we obtain an unbounded formal solution of the cKP1 equation, which corresponds to a line soliton (plane soliton with a straight-wise front) of the KP1 equation.[3] Such a solution can also be obtained through the relationship between the KP and cKP equation shown in Fig. 1 of Part I of this study.[1] Another choice of particular solutions is in the form of Airy functions,

$$\begin{aligned} \psi_l=\chi_l^*&=\frac{A_l}{\sqrt[3]{r}}\mathrm{Ai}\left(\frac{\tau-12\lambda_l}{\sqrt[3]{12r}}\right)e^{i\lambda_l\theta},\quad\text{or}\\ \psi_l=\chi_l^*&=\frac{B_l}{\sqrt[3]{r}}\mathrm{Bi}\left(\frac{\tau-12\lambda_l}{\sqrt[3]{12r}}\right)e^{i\lambda_l\theta}, \end{aligned} \tag{2.6}$$

where $\lambda_l$ is real parameter yield solutions in the form of Ai- and Bi-solitons, respectively, described in Part I. Due to the linearity of the Lax pair, a linear combination of solution (2.6) is also a solution,

$$\psi_l=\chi_l^*=\sum\left[\frac{A_l}{\sqrt[3]{r}}\mathrm{Ai}\left(\frac{\tau-12\lambda_l}{\sqrt[3]{12r}}\right)e^{i\lambda_l\theta}+\frac{B_l}{\sqrt[3]{r}}\mathrm{Bi}\left(\frac{\tau-12\lambda_l}{\sqrt[3]{12r}}\right)e^{i\lambda_l\theta}\right], \tag{2.7}$$

where $A_l$ and $B_l$ are arbitrary constants. Moreover, a derivative of solution (2.7) with respect to the parameter $\lambda_l$ is also a solution to

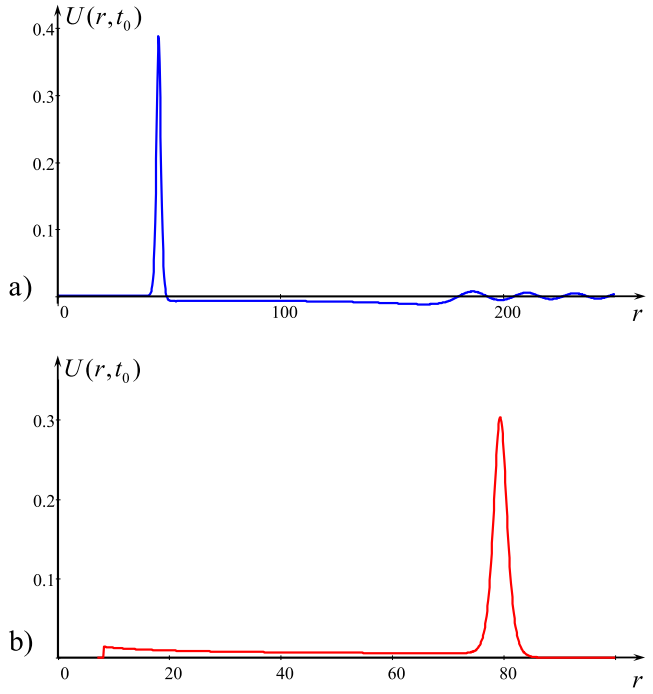


**FIG. 1.** Structure of Ai- and Bi-solitons in positive dispersion media. Frame (a) illustrates a typical Ai-soliton, and frame (b) illustrates a typical Bi-soliton. (A rear part of the Bi-soliton tail has been cut because it went to infinity when $r \to 0$, whereas, at the vicinity of $r = 0$, the cKP equation is inapplicable.)

the Lax pair with $U = 0, V = 0$,

$$\psi_l = \chi_l^* = \sum \left[ \frac{\partial}{\partial \lambda_l} \frac{A_l}{\sqrt[3]{r}} \mathrm{Ai}\left( \frac{\tau - 12\lambda_l}{\sqrt[3]{12r}} \right) e^{i\lambda_l \theta} + \frac{\partial}{\partial \lambda_l} \frac{B_l}{\sqrt[3]{r}} \mathrm{Bi}\left( \frac{\tau - 12\lambda_l}{\sqrt[3]{12r}} \right) e^{i\lambda_l \theta} \right]. \quad (2.8)$$

In a similar way, one can construct the $N$-soliton solution in terms of Airy functions of the first and second kinds by setting $p_l = 1$ and choosing appropriate functions (2.6). Many other particular solutions can be derived from Eqs. (2.7) and (2.8); however, not all of them are physically meaningful. Below, we discuss some solutions focusing basically on the most interesting and physically meaningful solutions.

## III. LUMP CHAINS

Soliton-type solutions containing Airy functions of the first and second kinds (Ai-solitons and Bi-solitons, respectively) have similar features. The big difference between these solitons is that in the positive dispersion media with $\sigma^2 = -1$, the pulse follows small-amplitude leading ripples and shelf in the Ai-solitons, whereas, in the Bi-solitons, a leading pulse is accompanied by a long small-amplitude shelf; this is illustrated by Fig. 1. [In this figure and all subsequent ones, we show $U(t, r, \varphi) = \alpha\, u(t, r, \varphi)/6$.]

An inspection of soliton solutions shows that Ai-solitons are described by a function that vanishes when $r \to \infty$, whereas Bi-solitons are described by a function that inevitably has a singularity at a very big distance from the pulse head (see Ref. 1). Perhaps, this singularity is not essential from a physical point of view and can be ignored because, at such big distances, soliton fields practically vanish; this issue remains open and requires further investigation and comparison with experimental and numerical data. Modulation instability of ring solitary waves in positive dispersion media develops similarly regardless of their initial structure. We will focus further primarily on the modulation instability of ring Ai-solitons; however, the results are the same if one replaces Ai-functions with Bi-functions in the subsequent formulas. As shown numerically in Part I of this study,[1] modulation instability of ring solitons with respect to azimuthal perturbations of their fronts leads to the emergence of lumps; in fact, the emergence of lump chains because even a single lump in a circular geometry represents a chain due to the periodicity of solutions in the angular variable. Here, we present analytical solutions describing the emergence of lump chains from ring solitons.

A solution representing a lump chain can be obtained if we set in Eq. (2.3) $p_l = 0$ and

$$\psi_l = \chi_l^* = \frac{A_{2l-1}}{\sqrt[3]{r}} \mathrm{Ai}\left( \frac{\tau - 12\lambda_{2l-1}}{\sqrt[3]{12r}} \right) e^{i\lambda_{2l-1}\theta} + \frac{A_{2l}}{\sqrt[3]{r}} \mathrm{Ai}\left( \frac{\tau - 12\lambda_{2l}}{\sqrt[3]{12r}} \right) e^{i\lambda_{2l}\theta}. \quad (3.1)$$

In this solution, the integration path in Eq. (2.5) is a ray extending from $\tau$ to $+\infty$. The number of lumps in each lump chain on the azimuthal interval $-\pi < \varphi \le \pi$ is determined by the difference between the parameters $\lambda$: $m_l = |\lambda_{2l} - \lambda_{2l-1}| \sqrt{6c\sigma^2\,(2/\beta c)^{1/3}}$. [Note that in a similar way, lump chains were obtained in the KP1 equation[10,11] with functions $f = \exp(\phi_1) + \exp(\phi_2)$ and $g = f^*$, where $\phi_j = \lambda_j x + i\lambda_j^2 y - 4\lambda_j^3 t$, and $\lambda_j$ being a complex parameter $(j = 1, 2)$.] The simplest chain with only one lump on the period can be obtained if we set $n = 1$ in Eq. (2.3). In general, the auxiliary function corresponding to the $m_1$-lump solution can be expressed as

$$\Gamma = \frac{\sqrt[3]{12}A_1^2}{\sqrt[3]{r}} \left\{ \left[ \mathrm{Ai}'(z_1) \right]^2 - z_1 \mathrm{Ai}(z_1)^2 \right\} + \frac{\sqrt[3]{12}A_2^2}{\sqrt[3]{r}} \times \left\{ \left[ \mathrm{Ai}'(z_2) \right]^2 - z_2 \mathrm{Ai}(z_2)^2 \right\} + \frac{2A_1A_2}{\sqrt[3]{12}\,(\lambda_2 - \lambda_1)} \times \left[ \mathrm{Ai}'(z_2)\,\mathrm{Ai}(z_1) - \mathrm{Ai}'(z_1)\,\mathrm{Ai}(z_2) \right] \cos\left[ (\lambda_1 - \lambda_2)\,\theta \right], \quad (3.2)$$

with $z_l = (\tau - 12\lambda_l)/\sqrt[3]{12r}$.

Due to the properties of Hirota's transformation, multiplying auxiliary function equation (3.2) by any constant factor does not affect the solution. Therefore, we can set $A_1 = 1$ and set for $A_2$ any nonzero real number in the interval $(-1, 1)$. Function (3.2) can be interpreted as an Ai-soliton controlled by the parameter $z_1$ that produces a lump chain under modulation of a ring wave controlled by the parameter $z_2$. When the perturbation is extremely small ($A_2 \to 0$), the resultant lump chain moves with a small velocity and consists of big-amplitude lumps. In another limit, when the perturbation is more pronounced, specifically when $|A_2| \to 1$, the

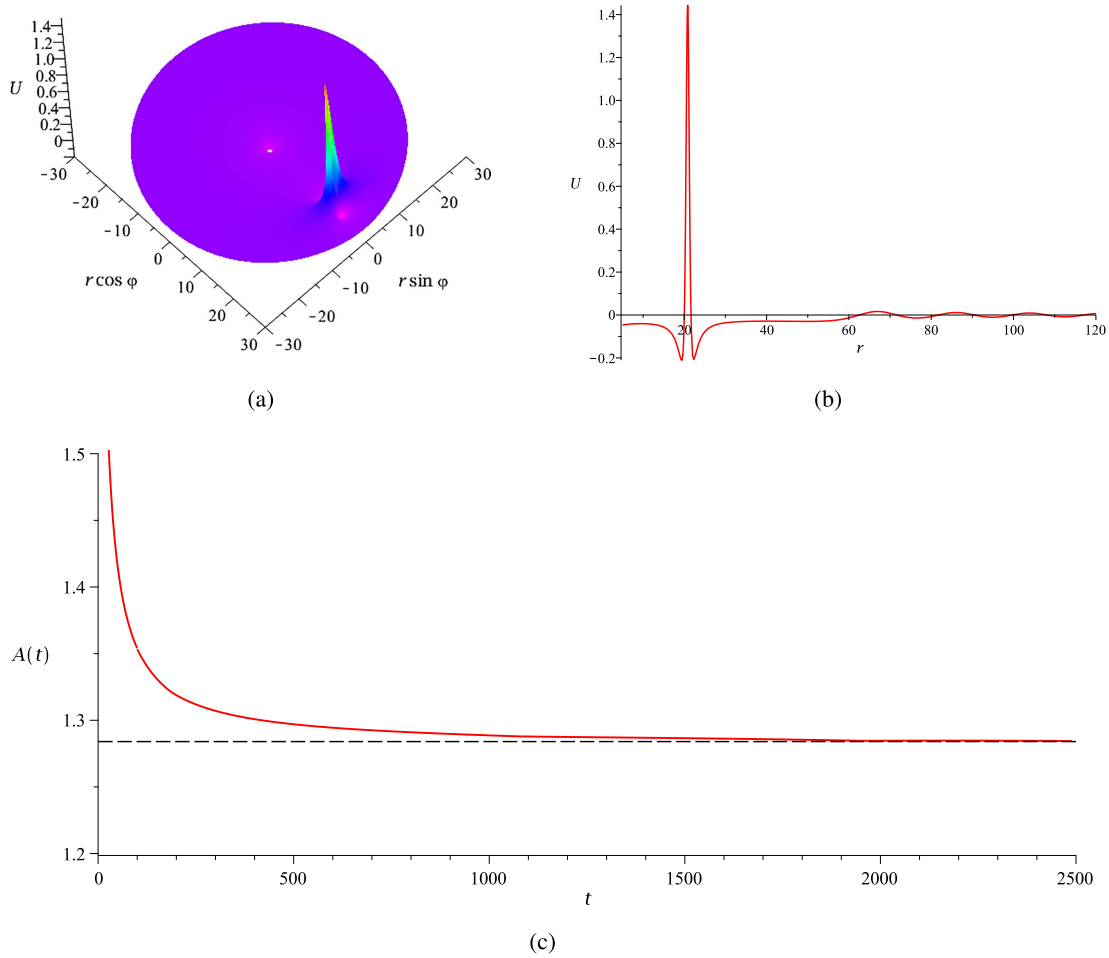


**FIG. 2.** A one-lump chain with only one lump on the period $-\pi < \varphi \le \pi$. The solution shown in panel (a) is described by the function (3.2) at $t = 40$ with the following parameters $\{A_1 = 1,\ A_2 = -1/4,\ \beta = -2,\ c = 1,\ \lambda_1 = 0,\ \lambda_2 = 1/\sqrt{6}\}$. Replacement of $A_2$ from $-1/4$ to $1/4$ with the same other parameters leads to the change of the directions of lump motion by $\pi$. Panel (b) shows a cross section of the lump at $\varphi = 0$. Panel (c) demonstrates a decrease of a lump amplitude and stabilization at $A = 1.284$ when $t \to +\infty$. The numerically obtained trajectory is well-approximated by a straight line $r = 0.51t + 0.50$ as $t \to +\infty$.

resultant lump chain moves faster but consists of small-amplitude lumps.

When $m_1 = 1$, the modulation effect is hardly visible, but as a result of its development, one lump emerges on the interval $-\pi < \varphi \le \pi$. Figure 2 presents a single lump, whose amplitude and velocity stabilize over time. The modulation instability looks clearer for bigger $m_1$ that plays the role of a mode number. In particular, when $m_1 = 4$, one can observe the development of the modulation instability shown in Fig. 3. At the early stage of modulation development, for $t < 3$, the amplitude of the carrier ring wave decreases, and the amplitude of modulation irregularly oscillates on its background. However, then, after $t = 3$, four spikes are created on the ring wave, and their amplitudes begin to increase. Eventually, four lumps emerge from spikes with gradually increasing amplitudes that approach constant values.

Solutions shown in Figs. 2 and 3 were obtained with small values of $A_2$ in comparison with $A_1$. In such cases, $A_2$ plays a role of a small parameter in expression (3.2), and then the approximate solution can be derived up to terms of $o(A_2)$,

$$U = 2\frac{\partial^2}{\partial\tau^2}\ln\Gamma_1 + 2\left(\frac{\partial^2}{\partial\tau^2}\frac{\Gamma_2}{\Gamma_1}\right)A_2 + O\left(A_2^2\right), \tag{3.3}$$

where

$$\Gamma_1 = \frac{\sqrt[3]{12}}{\sqrt[3]{r}}\left\{\left[\mathrm{Ai}'(z_1)\right]^2 - z_1\mathrm{Ai}(z_1)^2\right\},$$
$$\Gamma_2 = \frac{2}{\sqrt[3]{12}\,(\lambda_2 - \lambda_1)}\left[\mathrm{Ai}'(z_2)\,\mathrm{Ai}(z_1) - \mathrm{Ai}'(z_1)\,\mathrm{Ai}(z_2)\right] \tag{3.4}$$
$$\times\cos\left[(\lambda_1 - \lambda_2)\,\theta\right].$$

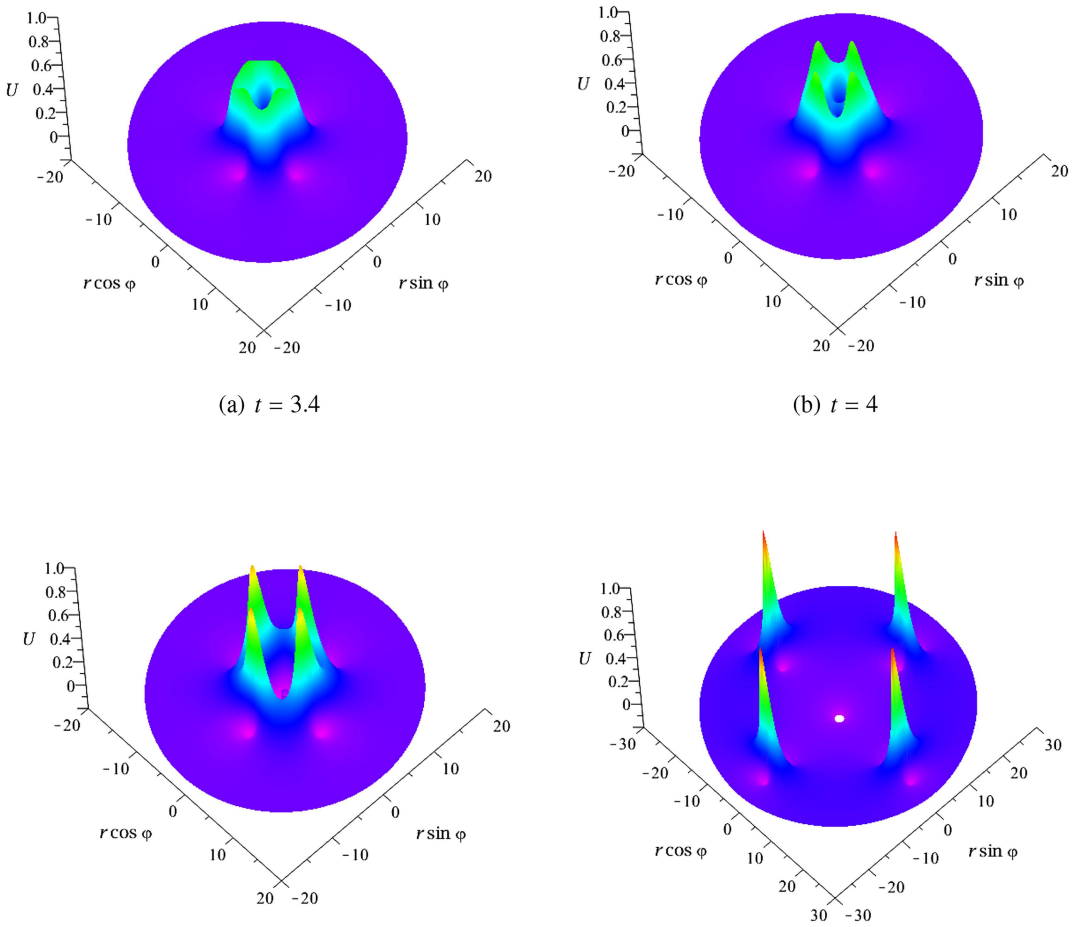


(a) $t = 3.4$ (b) $t = 4$

(c) $t = 6$ (d) $t = 30$

**FIG. 3.** Development of modulation instability when mode 4 azimuthal perturbation is imposed on the ring Ai-soliton. (a) $t = 3.4$, (b) $t = 4$, (c) $t = 6$, and (d) $t = 30$. The solution is plotted for the function (3.2) with the following parameters: $\{c = 1,\ \beta = -2,\ A_1 = 1,\ A_2 = -0.01,\ \lambda_1 = -2/\sqrt{6},\ \lambda_2 = 2/\sqrt{6}\}$. (a) $t = 3.4$. (b) $t = 4$. (c) $t = 6$. (d) $t = 30$.

In the limiting case $A_2 = 0$, Eq. (3.2) is identical to Eq. (2.4) in Part I,[1] which describes self-similar decaying circular ripples derived first by Johnson.[2] However, when $A_2 = 1$, Eq. (3.2) describes ripples composed of countless lump-type chains, each consisting of $m_1$ lump waves. Moreover, as $m_1$ increases, the manifestation of lump waves becomes more pronounced, as shown in Fig. 4. Amplitudes of lump-type formation decay with time.

The interaction between any number of lump chains can be expressed through the following auxiliary function:

$$\Gamma = \begin{vmatrix} \Theta_{11} & \Theta_{12} & \cdots & \cdots & \Theta_{1,N} \\ \Theta_{21} & \Theta_{22} & \cdots & \cdots & \Theta_{2,N} \\ \vdots & \vdots & \ddots & & \vdots \\ \vdots & \vdots & & \ddots & \vdots \\ \Theta_{N,1} & \Theta_{N,2} & \cdots & \cdots & \Theta_{N,N} \end{vmatrix}, \tag{3.5}$$

where

$$\Theta_{lj} = \Omega_{2l-1,2j-1} + \Omega_{2l-1,2j} + \Omega_{2l,2j-1} + \Omega_{2l,2j}, \tag{3.6}$$

$$\Omega_{l,l} = \frac{\sqrt[3]{12}A_l^2}{\sqrt[3]{r}} \left\{ \left[ \mathrm{Ai}'(z_l) \right]^2 - z_l \mathrm{Ai}(z_l)^2 \right\}, \tag{3.7}$$

$$\Omega_{l,j} = \frac{A_j A_l}{\sqrt[3]{12}\left(\lambda_j - \lambda_l\right)} \left[ \mathrm{Ai}^{(1)}\left(z_j\right) \mathrm{Ai}\left(z_l\right) - \mathrm{Ai}^{(1)}\left(z_l\right) \mathrm{Ai}\left(z_j\right) \right] \mathrm{e}^{-i(\lambda_j - \lambda_l)\theta}.$$

An example of the interaction between two lump chains is depicted in Fig. 5, where the high-amplitude lump chain consists of a single lump on a period (this chain is controlled by the parameters $A_1$, $A_2$, $\lambda_1$, and $\lambda_2$), while the low-amplitude lump chain consists of five lumps on a period. The low-amplitude lump chain propagates faster; therefore, it overtakes a single lump and interacts with it. The interaction is elastic so that both lump chains re-appear after

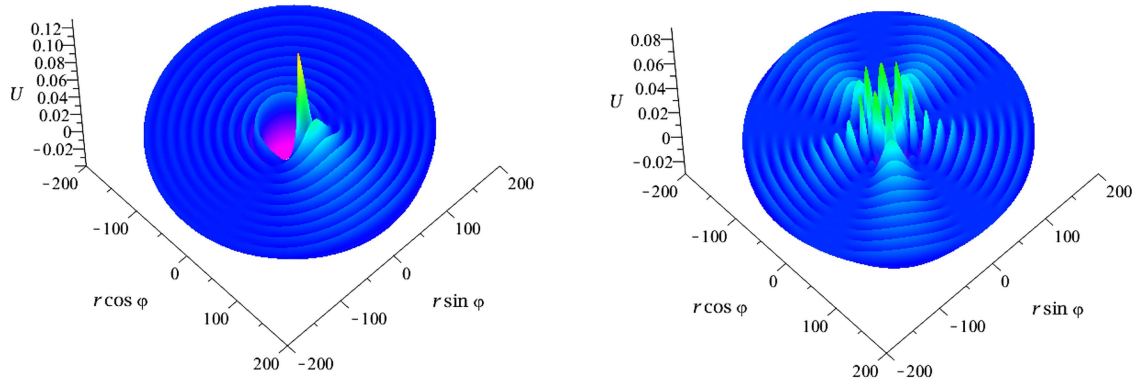


(a) $m_1 = 1$ (b) $m_1 = 5$

**FIG. 4.** Ripplon solutions at $t = 20$ that are described by the auxiliary function (3.2) with $A_1 = -A_2 = 1$ and $c = 1$, $\beta = -2$. In panel (a), there is only one lump when the following parameters are chosen $\lambda_1 = 0$, $\lambda_2 = -1/\sqrt{6}$. In panel (b), five primary lumps exist close to the center and a series of quasi-lump formations in front of each lump when the following parameters are chosen $\lambda_1 = 3/\sqrt{6}$, $\lambda_2 = -2/\sqrt{6}$. (a) $m_1 = 1$. (b) $m_1 = 5$.

the interaction even without a shift in the angular direction. In this particular case with the lump amplitude ratio $A_1/A_2 = 5.42/0.81 = 6.69 > 3$, the interaction has an overtaking character. However, a similar overtaking character occurs even when the amplitude ratio of lumps is less than 2.

## IV. THE INTERACTION OF A LUMP CHAIN WITH A RING SOLITON

In this section, we consider a solution describing a "normal," non-resonant interaction of a lump chain and a ring wave in the form of the Ai-soliton (a similar solution can be obtained if we replace an Ai-soliton by a Bi-soliton). In such an interaction, both structures, the lump chain and the ring soliton, re-appear after the interaction albeit with different amplitudes due to the cylindrical divergence. In Sec. V, we present solutions describing "abnormal" resonant interactions between various structures.

A hybrid solution consisting of a lump chain and a ring wave can be expressed through the following auxiliary function:

$$\Gamma = \begin{vmatrix} \langle \psi_1, \chi_1 \rangle & \langle \psi_1, \chi_2 \rangle \\ \langle \psi_2, \chi_1 \rangle & 1 + \langle \psi_2, \chi_2 \rangle \end{vmatrix} = \begin{vmatrix} \Omega_{11} + \Omega_{12} + \Omega_{21} + \Omega_{22} & \Omega_{13} + \Omega_{23} \\ \Omega_{31} + \Omega_{32} & 1 + \Omega_{33} \end{vmatrix}, \tag{4.1}$$

where

$$\psi_1 = \chi_1^* = \frac{A_1}{\sqrt[3]{r}} \mathrm{Ai}\left( \frac{t - 12\lambda_1}{\sqrt[3]{12r}} \right) e^{i\lambda_1 \theta} + \frac{A_2}{\sqrt[3]{r}} \mathrm{Ai}\left( \frac{t - 12\lambda_2}{\sqrt[3]{12r}} \right) e^{i\lambda_2 \theta}, \tag{4.2}$$

$$\psi_2 = \chi_2^* = \frac{A_3}{\sqrt[3]{r}} \mathrm{Ai}\left( \frac{t - 12\lambda_3}{\sqrt[3]{12r}} \right) e^{i\lambda_3 \theta}.$$

Here, functions $\Omega_{i,j}$ are those that are given in Eq. (3.7).

The interaction of a lump chain with a circular wave can be classified into two types based on whether the lump chain undergoes displacement on the angular variable in the course of interaction or not. We explain these two cases through the interaction of the simplest lump chain with only one lump on a period and a circular wave.

Figure 6 illustrates the energy exchange interaction between a lump chain and a circular wave. Panel (a) shows the initial state, where a slow moving lump of a big amplitude is located in front of a faster-moving circular soliton of a smaller amplitude. As time progresses, the amplitude of the circular wave continuously decreases, and its speed increases. On the front of a ring wave, a localized perturbation (a spike) appears and gradually grows when the ring wave approaches the lump [see panels (b) and (c) in Fig. 6]. This perturbation ultimately evolves into a lump of a big amplitude, which moves slower than the ring wave and lags behind its front [see panels (c) and (d) in Fig. 6]. At the same time, the initial lump that was in front of the ring wave loses its energy, decreases in amplitude, and is eventually absorbed by the ring soliton.

There is also another type of interaction of a lump chain and a ring soliton, which is illustrated by Fig. 7. When a small-amplitude circular wave approaches a lump, they merge with each other at the point of contact as shown in panels (b) and (c) of Fig. 7. Meanwhile, a spike arises on the front of a ring soliton at the opposite side (on half a period of the lump chain). The spike grows with time and evolves into a big-amplitude lump that lags from the soliton front, whereas the initial lump dissolves in the ring soliton. This process can be interpreted as the phase shift of a lump chain along the azimuthal coordinate $\varphi$ on half of a period as a result of interaction with a ring soliton.

Both of the aforementioned interactions are elastic. Note that if $A_3 = 0$ in the solutions considered above, then under the same other parameters used in Figs. 6 and 7, we obtain a lump chain with a single lump whose amplitude asymptotically approaches $A_\infty = 2.16$. The lumps move along the ray $\varphi = 0$. However, if $A_3 \neq 0$ as in Figs. 6 and 7, then ring solitons asymptotically disappear as their

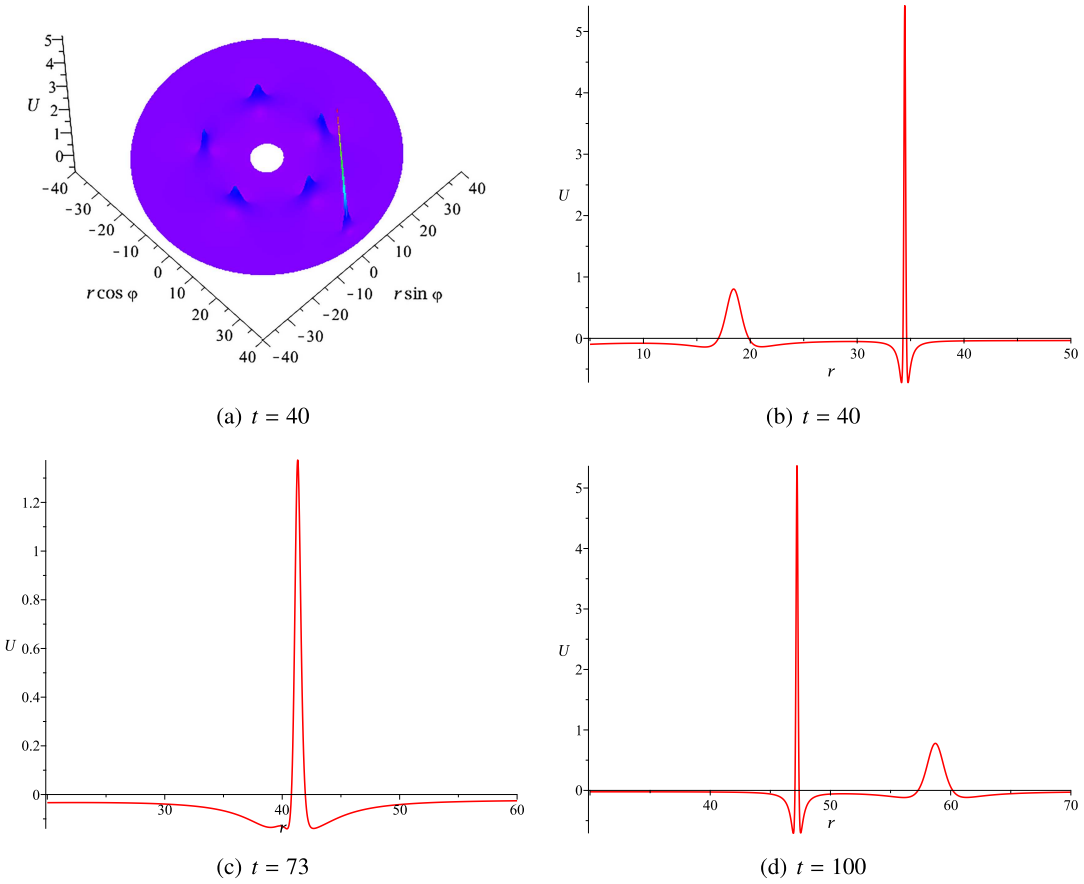


**FIG. 5.** The interaction between two lump chains described by the auxiliary equation (3.5) with the following parameter choice $\{c = 1,\ \beta = -2,\ A_1 = 1,\ A_2 = -1/15,\ A_3 = 1,\ A_4 = -1/200,\ \lambda_1 = -25/\sqrt{6},\ \lambda_2 = -24/\sqrt{6},\ \lambda_3 = 1/\sqrt{6},\ \lambda_4 = \sqrt{6}\}$. Panel (a): Three-dimensional plot; panels (b)–(d) cross sections at $\varphi = 0$. (a) $t = 40$. (b) $t = 40$. (c) $t = 73$. (d) $t = 100$.

amplitudes gradually decrease $A_r \sim r^{-2/3}$, whereas lumps stabilize and move with the constant amplitudes $A_\infty = 2.16$.

In general, the interaction of $n_1$ lump chains and $n_2$ ring solitons can be described by the auxiliary function (2.3) with

$$\psi_l = \chi_l^* = \frac{A_{2l-1}}{\sqrt[3]{r}}\mathrm{Ai}\left(\frac{\tau - 12\lambda_{2l-1}}{\sqrt[3]{12r}}\right)e^{i\lambda_{2l-1}\theta} + \frac{A_{2l}}{\sqrt[3]{r}}\mathrm{Ai}\left(\frac{\tau - 12\lambda_{2l}}{\sqrt[3]{12r}}\right)e^{i\lambda_{2l}\theta}, \quad l \le n_1,$$
$$\psi_j = \chi_j^* = \frac{A_j}{\sqrt[3]{r}}\mathrm{Ai}\left(\frac{t - 12\lambda_j}{\sqrt[3]{12r}}\right)e^{i\lambda_j\theta}, \quad 2n_1 < j \le 2n_1 + n_2. \tag{4.3}$$

## V. RESONANT SOLUTIONS

In this subsection, we present the "abnormal," alias resonant, interactions of lump chains and ring solitons. Abnormal interactions pertain to the cases when nonlinear entities (solitons or lumps) do not re-emerge after the interaction with each other or when they emerge from other entities or, inversely, can be absorbed by other entities. The abnormal interaction caused by velocity resonance results in slower changes in the distances between the interacting solitary waves compared to normal interactions.[12–14] On the other hand, the interaction caused by an infinite phase shift during collisions leads to significantly more complicated changes in the distance between entities; for instance, this can give rise to the formation of $Y$-shaped solitons or stable $Y$-shaped lump chains that move at a constant speed. Additionally, this can lead to the creation of resonances between two weakly interacting plane waves and transient lumps.[11,15,16] We start with the simplest case of such an interaction, which describes the absorption of a lump chain by a ring soliton. This is a cylindrical analog of resonant interaction known for the conventional KP1 equation.[6,10,11]

### A. Absorption of a lump chain by a ring soliton

This type of resonant interaction is described by the auxiliary function (2.4) with $n = 1$, $p_1 > 0$, and functions $\psi_1$ and $\chi_1$ presented by Eq. (3.1). The explicit form of the auxiliary function $\Gamma$

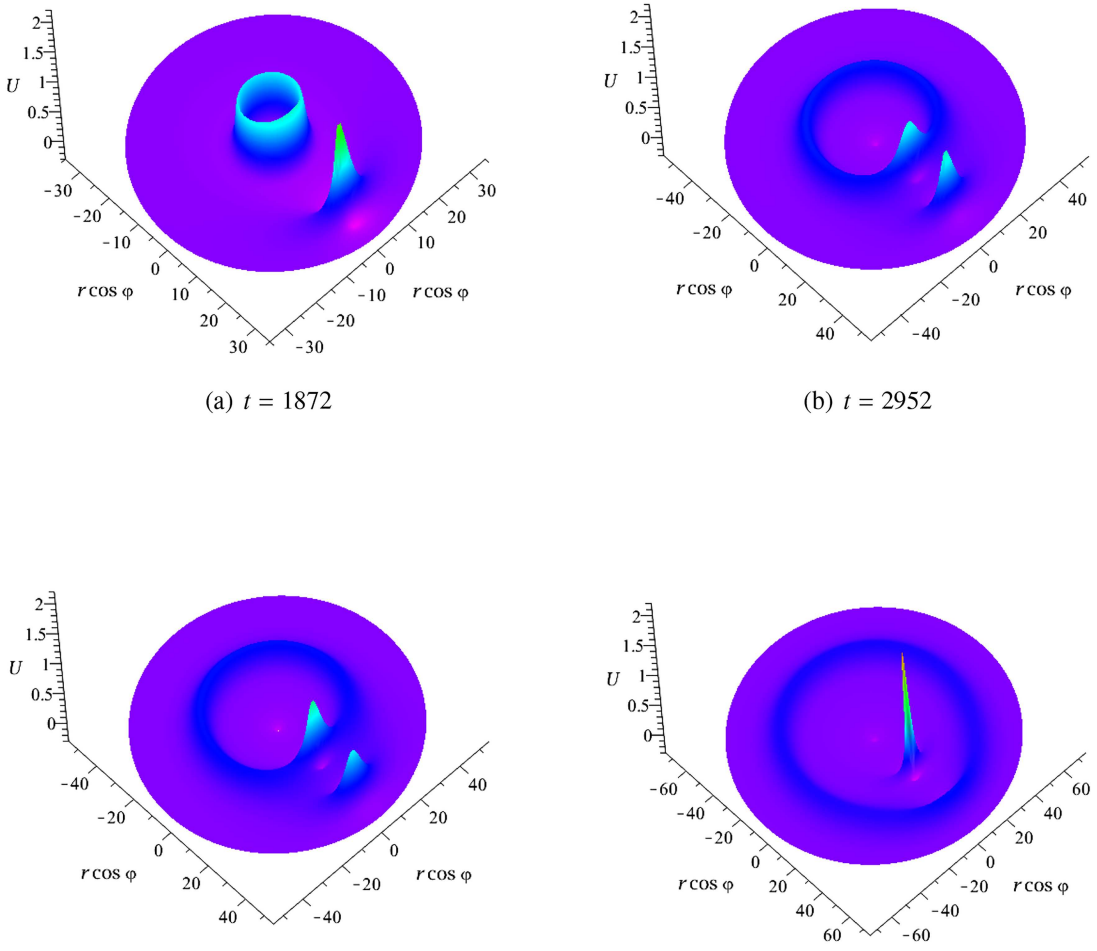


(a) $t = 1872$ (b) $t = 2952$

(c) $t = 3096$ (d) $t = 3816$

**FIG. 6.** The exchange interaction between a lump chain consisting of only one lump on a period and a ring wave. (a) $t = 1872$, (b) $t = 2952$, (c) $t = 3096$, and (d) $t = 3816$. This solution was generated through the auxiliary function (4.1) with the following parameters: $\{c = 1/12,\ \beta = -3,\ A_1 = 1,\ A_2 = -1/80,\ A_3 = 10^7,\ \lambda_1 = 0,\ \lambda_2 = 1,\ \lambda_3 = -1/2\}$. (a) $t = 1872$. (b) $t = 2952$. (c) $t = 3096$. (d) $t = 3816$.

in this case is

$$\Gamma = p_1 + \frac{\sqrt[3]{12}A_1^2}{\sqrt[3]{r}}\left\{\left[\mathrm{Ai}'(z_1)\right]^2 - z_1\mathrm{Ai}(z_1)^2\right\} + \frac{\sqrt[3]{12}A_2^2}{\sqrt[3]{r}} \times \left\{\left[\mathrm{Ai}'(z_2)\right]^2 - z_2\mathrm{Ai}(z_2)^2\right\} + \frac{2A_1A_2}{\sqrt[3]{12}(\lambda_2 - \lambda_1)} \times \left[\mathrm{Ai}'(z_2)\,\mathrm{Ai}(z_1) - \mathrm{Ai}'(z_1)\,\mathrm{Ai}(z_2)\right]\cos\left[(\lambda_1 - \lambda_2)\theta\right], \quad (5.1)$$

where $A_1 = 1$, $A_2$ is any nonzero real number from the interval $(-1,\ 1)$ and $0 < p_1 \lll A_1$. [A solution with $A_2 = 1$ describes a decaying ripplon (see Fig. 4) instead of a constant-amplitude lump chain.]

The resonance phenomenon described by Eq. (5.1) looks as follows. At the initial moment, there is a gradually decaying circular soliton moving outward; its amplitude decays as $A \sim r^{-2/3}$. In front of the cylindrical soliton at some distance, there is a lump chain composed of $m_1 = |\lambda_2 - \lambda_1|\sqrt{6c\sigma^2\,(2/\beta c)^{1/3}}$ lumps as shown in Fig. 8(a). As time elapses, a ring soliton that moves faster than the lump chain approaches the chain and merges with it [see Figs. 8(b) and 8(c)]. Then, the lumps sitting on the soliton gradually dissolve in it, and only a circular soliton further moves at infinity as shown in Fig. 8(d).

## B. Emission of a lump chain by a ring soliton

There is an inverse phenomenon when a ring soliton emits a lump chain. This process is described by the following auxiliary

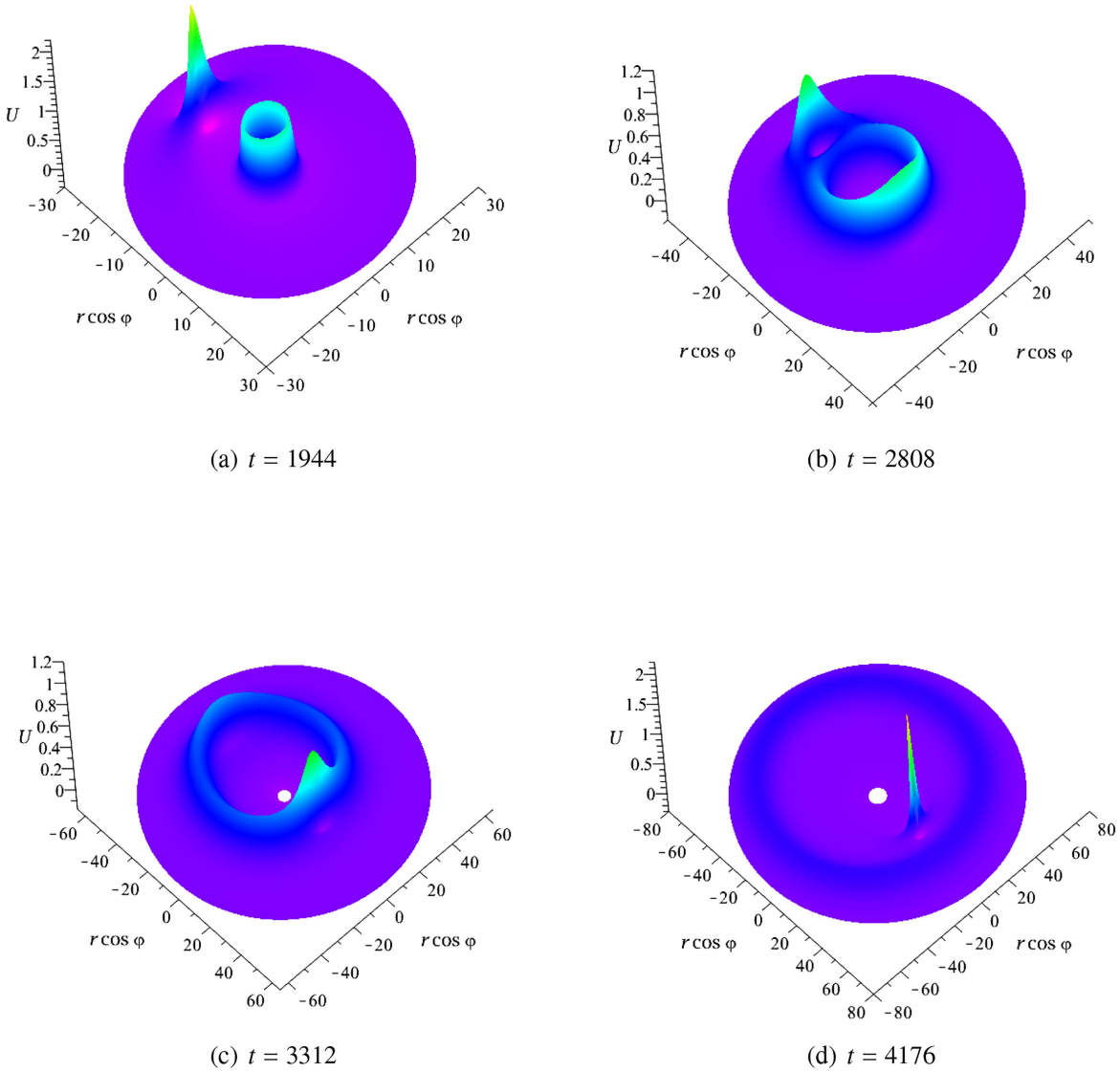


(a) $t = 1944$ (b) $t = 2808$

(c) $t = 3312$ (d) $t = 4176$

**FIG. 7.** The adsorption–extraction interaction between a lump chain consisting of only one lump on a period and a ring wave. (a) $t = 1944$, (b) $t = 2808$, (c) $t = 3312$, and (d) $t = 4176$. This solution was generated through the auxiliary function (4.1) with the following parameters: $\{c = 1/12,\ \beta = -3,\ A_1 = 1,\ A_2 = -1/80,\ A_3 = 10^6,\ \lambda_1 = 0,\ \lambda_2 = 1,\ \lambda_3 = 1/3\}$. (a) $t = 1944$. (b) $t = 2808$. (c) $t = 3312$. (d) $t = 4176$.

function:

$$\begin{aligned}\Gamma &= \begin{vmatrix} \langle \psi_1, \chi_1 \rangle & \langle \psi_1, \chi_2 \rangle \\ \langle \psi_2, \chi_1 \rangle & 1 + \langle \psi_2, \chi_2 \rangle \end{vmatrix} \\ &= \begin{vmatrix} \Omega_{11} + \Omega_{12} + \Omega_{21} + \Omega_{22} & \Omega_{11} + \Omega_{21} \\ \Omega_{11} + \Omega_{12} & p_2 + \Omega_{11} \end{vmatrix}, \\ &= p_2 (\Omega_{11} + \Omega_{12} + \Omega_{21}) + \Omega_{22}\Omega_{11} - \Omega_{21}\Omega_{12} + \Omega_{22}, \end{aligned} \tag{5.2}$$

with

$$\begin{aligned}\psi_1 = \chi_1^* &= \frac{A_1}{\sqrt[3]{r}} \mathrm{Ai}\left(\frac{t - 12\lambda_1}{\sqrt[3]{12r}}\right) e^{i\lambda_1 \theta} + \frac{A_2}{\sqrt[3]{r}} \mathrm{Ai}\left(\frac{t - 12\lambda_2}{\sqrt[3]{12r}}\right) e^{i\lambda_2 \theta}, \\ \psi_2 = \chi_2^* &= \frac{A_1}{\sqrt[3]{r}} \mathrm{Ai}\left(\frac{t - 12\lambda_1}{\sqrt[3]{12r}}\right) e^{i\lambda_1 \theta}, \end{aligned} \tag{5.3}$$

where $A_1 = 1$, $A_2$ is any nonzero real number from the interval $(-1,\ 1)$, $0 < p_2 \lll A_1$, and functions $\Omega_{lj}$ are given in Eq. (3.7).

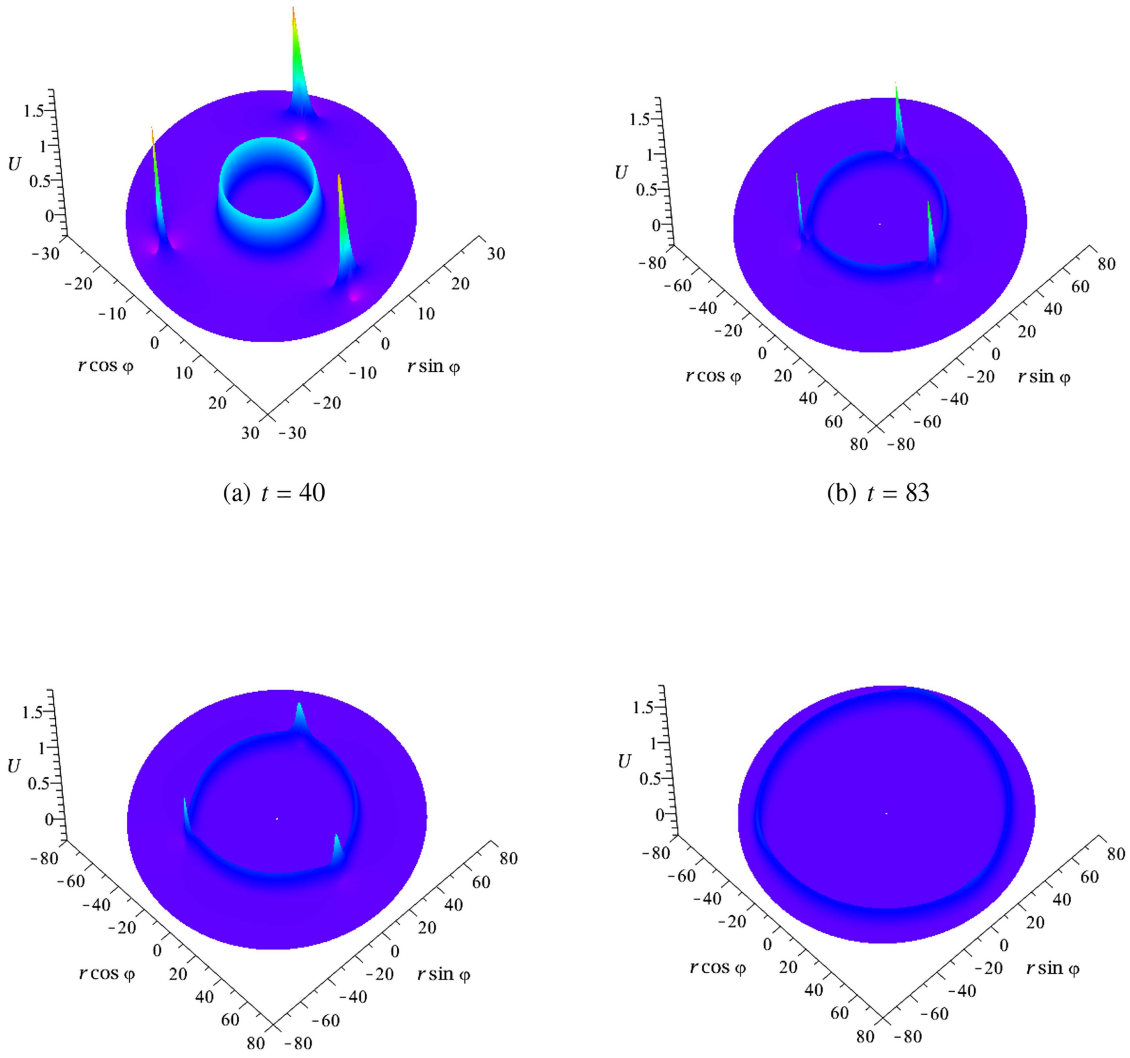


(a) $t = 40$ (b) $t = 83$

(c) $t = 93$ (d) $t = 125$

**FIG. 8.** Absorption of a lump chain by a circular soliton; the process described by Eq. (5.1) with the following parameters $\{c = 1,\ \beta = -2,\ A_1 = 1,\ A_2 = -10^{-2},\ \lambda_1 = -3/\sqrt{6},\ \lambda_2 = 0,\ p_1 = 10^{-15}\}$. (a) $t = 40$, (b) $t = 83$, (c) $t = 93$, and (d) $t = 125$. (a) $t = 40$. (b) $t = 83$. (c) $t = 93$. (d) $t = 125$.

The resonance phenomenon described by Eq. (5.2) looks as follows. At the initial moment, there is only a gradually decaying circular soliton moving outward; its amplitude decays as $A \sim r^{-2/3}$; this is shown in Fig. 9(a). As time elapses, a few spikes $m_1 = |\lambda_2 - \lambda_1|\sqrt{6c\sigma^2\,(2/\beta c)^{1/3}}$ gradually emerge on the soliton; the spikes are equally spaced on the soliton front. The spikes gradually evolve into lumps of big amplitudes that move slower than the small-amplitude ring soliton. Lumps and solitons separate from each other and move further independently as shown in Fig. 9.

### C. Fusion of two lump chains

Resonance can also occur between circular lump chains. This process is described by Eq. (2.3), with $N = 1$, $p_1 = 0$, and

$$\psi_1 = \chi_1^* = \frac{A_1}{\sqrt[3]{r}}\mathrm{Ai}\left(\frac{t - 12\lambda_1}{\sqrt[3]{12r}}\right)e^{i\lambda_1\theta} + \frac{A_2}{\sqrt[3]{r}}\mathrm{Ai}\left(\frac{t - 12\lambda_2}{\sqrt[3]{12r}}\right)e^{i\lambda_2\theta} + \frac{A_3}{\sqrt[3]{r}}\mathrm{Ai}\left(\frac{t - 12\lambda_3}{\sqrt[3]{12r}}\right)e^{i\lambda_3\theta}. \tag{5.4}$$

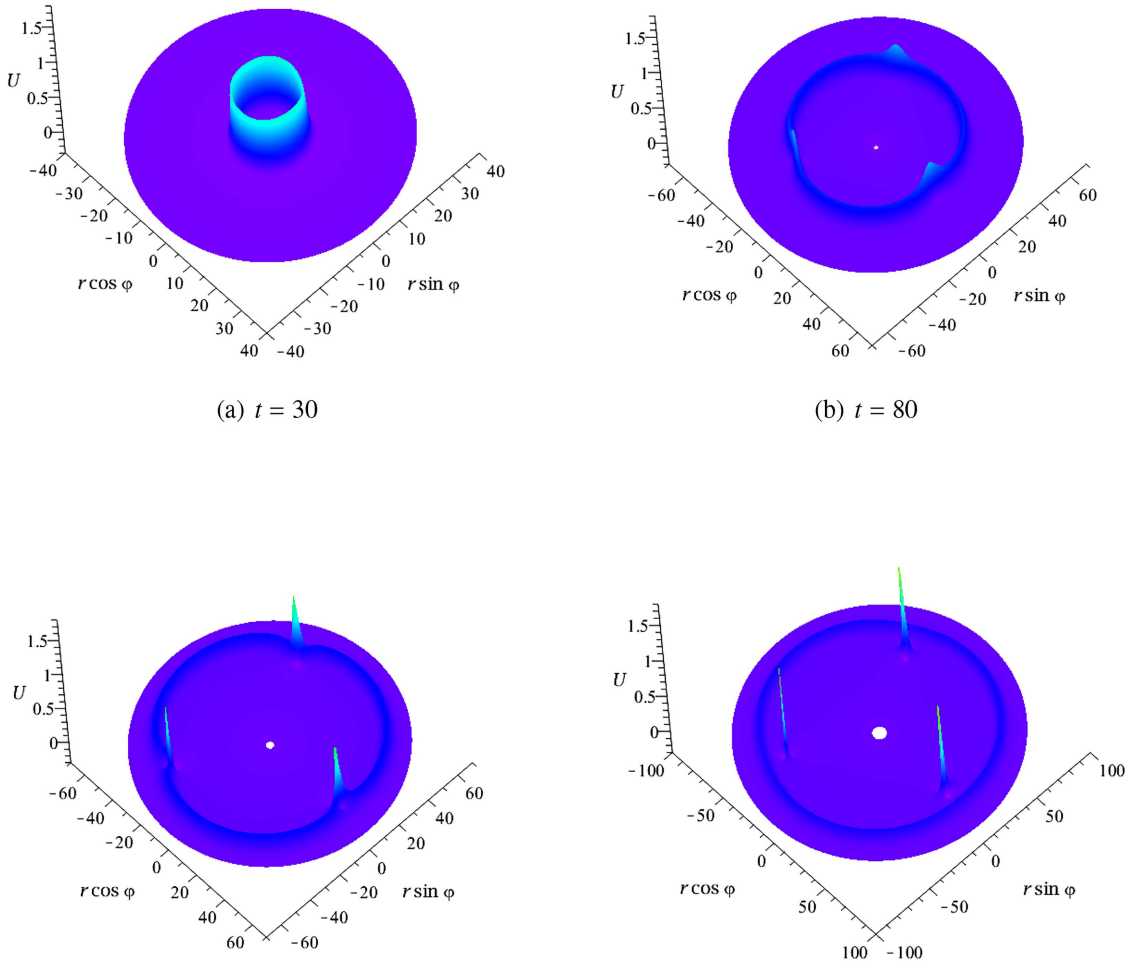


(a) $t = 30$ (b) $t = 80$

(c) $t = 100$ (d) $t = 130$

**FIG. 9.** The circular wave has emitted a chain composed of three lump waves: Eq. (5.2) with parameter selection $\{c = 1,\ \beta = -2,\ A_1 = 1,\ A_2 = -10^{-2},\ \lambda_1 = -3/\sqrt{6},\ \lambda_2 = 0,\ p_1 = 10^{-15}\}$. (a) $t = 30$, (b) $t = 80$, (c) $t = 100$, and (d) $t = 130$. (a) $t = 30$. (b) $t = 80$. (c) $t = 100$. (d) $t = 130$.

The auxiliary function corresponding to this resonance phenomenon can be expressed as follows:

$$\Gamma = \Omega_{11} + \Omega_{12} + \Omega_{13} + \Omega_{21} + \Omega_{22} + \Omega_{23} + \Omega_{31} + \Omega_{32} + \Omega_{33}, \tag{5.5}$$

where $\Omega_{ij}$ are given by Eq. (3.7). Figure 10 illustrates this resonance phenomenon. At $t = 3672$, a lump chain consisting of three lumps of a smaller amplitude $A = 0.65$ is located closer to the center. The lumps are equally spaced on the azimuthal variable where $\varphi = \pm\pi/3$ and $\pi$. Another lump chain consisting of two lumps with the amplitude 1.56 is located further from the center at the angles $\varphi = \pm\pi/2$ [see Fig. 10(a)]. As time elapses, the faster-moving three-lump chain gradually approaches the slower-moving two lump chains and merges with it as shown in panels (b) and (c). The amplitude of the two lump chains gradually decreases, while the amplitude of the three-lump chain gradually increases. Eventually, a five-lump chain forms with equally spaced lumps of equal amplitudes 1.18, as shown in Fig. 10(d).

### D. Fission of a lump chain onto two lump chains

The inverse effect to the lump chain fusion, the fission of a lump chain onto two lump chains, is described by the following auxiliary function:

$$\Gamma = \begin{vmatrix} \langle \psi_1, \chi_1 \rangle & \langle \psi_1, \chi_2 \rangle \\ \langle \psi_2, \chi_1 \rangle & \langle \psi_2, \chi_2 \rangle \end{vmatrix} \tag{5.6}$$

$$= \begin{vmatrix} \Omega_{11} + \Omega_{12} + \Omega_{21} + \Omega_{22} & \Omega_{12} + \Omega_{13} + \Omega_{22} + \Omega_{23} \\ \Omega_{21} + \Omega_{22} + \Omega_{31} + \Omega_{32} & \Omega_{22} + \Omega_{23} + \Omega_{32} + \Omega_{33} \end{vmatrix},$$

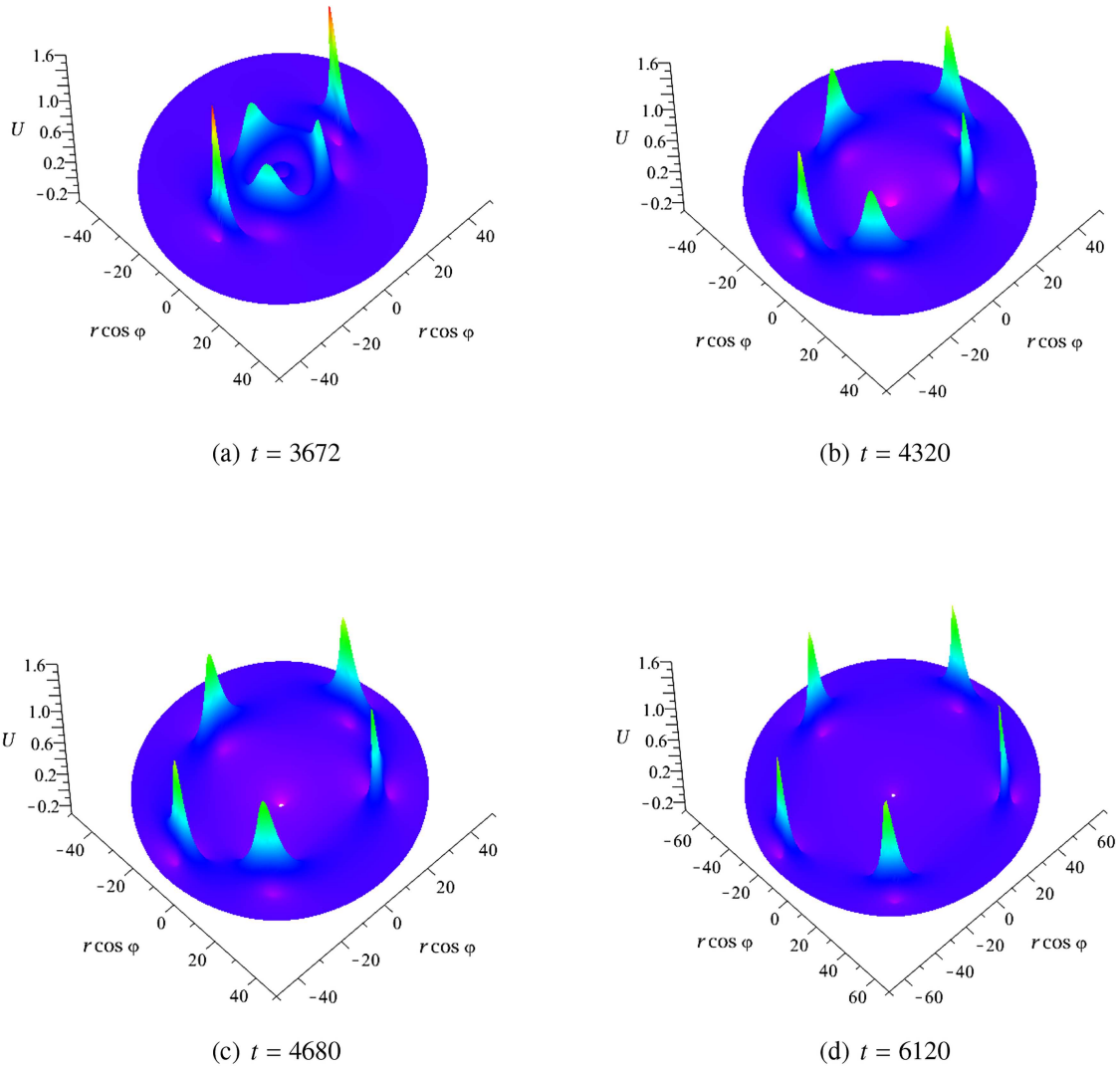


(a) $t = 3672$ (b) $t = 4320$

(c) $t = 4680$ (d) $t = 6120$

**FIG. 10.** Fusion of two lump chains described by the auxiliary function (5.5) with the following parameters $\{c = 1/12,\ \beta = -3,\ A_1 = 1,\ A_2 = (1/3)\cdot 10^{-3},\ A_3 = 10^{-7},\ \lambda_1 = 0,\ \lambda_2 = 2,\ \lambda_3 = 5\}$. (a) $t = 3672$, (b) $t = 4320$, (c) $t = 4680$, and (d) $t = 6120$. (a) $t = 3672$. (b) $t = 4320$. (c) $t = 4680$. (d) $t = 6120$.

where $\Omega_{lj}$ are the same function given by Eq. (3.7) with

$$\psi_1 = \chi_1^* = \frac{A_1}{\sqrt[3]{r}}\mathrm{Ai}\left(\frac{t-12\lambda_1}{\sqrt[3]{12r}}\right)e^{i\lambda_1\theta} + \frac{A_2}{\sqrt[3]{r}}\mathrm{Ai}\left(\frac{t-12\lambda_2}{\sqrt[3]{12r}}\right)e^{i\lambda_2\theta},$$
$$\psi_2 = \chi_2^* = \frac{A_2}{\sqrt[3]{r}}\mathrm{Ai}\left(\frac{t-12\lambda_2}{\sqrt[3]{12r}}\right)e^{i\lambda_2\theta} + \frac{A_3}{\sqrt[3]{r}}\mathrm{Ai}\left(\frac{t-12\lambda_3}{\sqrt[3]{12r}}\right)e^{i\lambda_3\theta}. \tag{5.7}$$

Figure 11 illustrates the process of the original chain disintegration onto two lump chains based on the auxiliary function (5.6). In panel (a), a lump chain with an amplitude of 1.10 and a period of $2\pi/5$ is shown at $t = 2448$. However, there is a hidden small perturbation that becomes gradually developing. As time progresses, the amplitudes of two lumps gradually increase, while the amplitudes of the other three lumps slowly decrease as shown in panels (b) and (c). The amplitudes of growing lumps eventually increase up to 1.95, while the amplitudes of decreasing lumps stabilize at 0.72.

Lumps with different amplitudes move at different speeds so that small-amplitude lumps move ahead. Thus, asymptotically, two equally spaced chains are formed, outer with three lumps, and inner with two lumps. This process resembles plane chain disintegration within the conventional KP1 equation.[6,10,11]

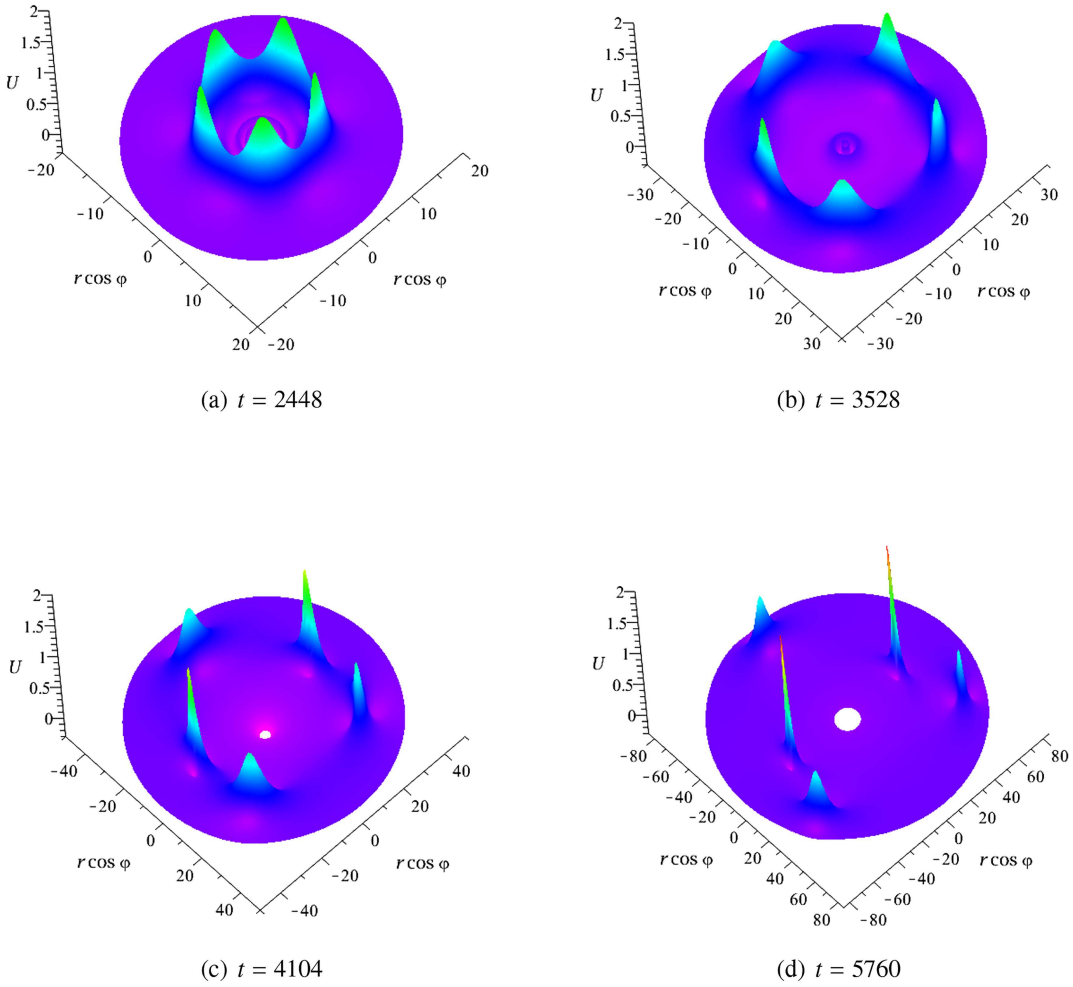


(a) $t = 2448$ (b) $t = 3528$

(c) $t = 4104$ (d) $t = 5760$

**FIG. 11.** Fusion of a lump chain onto two lump chains described by the auxiliary function (5.6) with the following parameters $\{c = 1/12,\ \beta = -3,\ A_1 = 1,\ A_2 = (1/3) \cdot 10^{-3},\ A_3 = 10^{-7},\ \lambda_1 = 0,\ \lambda_2 = 2,\ \lambda_3 = 5\}$. (a) $t = 2448$, (b) $t = 3528$, (c) $t = 4104$, and (d) $t = 5760$. (a) $t = 2448$. (b) $t = 3528$. (c) $t = 4104$. (d) $t = 5760$.

## VI. CONCLUSION

In two parts of this study, we investigated solutions to the cylindrical Kadomtsev–Petviashvili equation. It was demonstrated that physically meaningful solutions should be presented in the original variables [see Eq. (1.1)]; otherwise, solutions presented in the "standard variables," Eq. (1.2), can be confusing and not satisfying boundary conditions.[3] In Part I of this study,[1] we studied axisymmetric solutions and presented two types of soliton solutions described by Airy functions of the first and second kinds, the Ai- and Bi-solitons derived for the first time by Calogero and Degasperis[17,18] and Nakamura and Chen.[19] Such solutions are described by the cylindrical Kortweg–de Vries equation, which is a reduced version of the cKP equation. Following Calogero and Degasperis,[17] we call these solutions "solitons" as they wrote that solutions that they constructed "are in some sense the analogous of the single-soliton solutions (although they are not quite localized, having a slowly vanishing wiggling tail)." Our analysis shows that they really have many features of KdV solitons. We also presented self-similar solutions to the cKdV equation earlier derived by Johnson in application to the water wave theory.[2,20]

Ring solitons are subject to modulation instability with respect to the azimuthal variable in media with positive dispersion. Our estimates and numerical modeling have confirmed that the instability indeed occurs, and in the course of its development, a chain of fully localized two-dimensional structures (lumps) emerge from a circular soliton front. In Part II of our study, by means of the Darboux–Matveev transform,[3] we found an exact solution describing lump creation. Then, we found many other interesting solutions describing "normal" and "anomalous" interactions of lump chains with each other and with ring solitons. In addition to that, we also derived solutions describing decaying lumps and lump chains of complex spatial structure dubbed ripplons. All these solutions can

be relevant to many physical situations when nonlinear waves propagate in media with positive dispersion (plasma, solids, membranes, etc.).

In the conclusion, we list several issues that can be studied in the nearest perspective. Among them, the existence of multi-lump structures, such as those that were found in the conventional KP1 equation,[21–24] and normal and anomalous interactions between various structures.[10–16,22] Separately, we can mention a study of converging waves in the cylindrical geometry. This problem is topical for plasma wave experiments.[25,26] According to the preliminary consideration,[27] in such a case, one can expect modulation instability of converging circular waves even in media with negative dispersion. This study can be further extended to the important cases of physical significance but not described by completely integrable equations, such as the cylindrical Benjamin–Ono, modified Korteweg–de Vries equations, the spherical Korteweg–de Vries equation, etc. At least, asymptotic and numerical methods can shed light on the dynamics of nonlinear waves in such cases.

## ACKNOWLEDGMENTS

Qi Guo and Zhao Zhang acknowledge the financial support provided by the Natural Science Foundation of Guangdong Province of China (Grant No. 2021A1515012214) and the Science and Technology Program of Guangzhou (Grant No. 2019050001). Wencheng Hu acknowledges the funding provided by the China Scholarship Council (Grant No. 202002425001). Yury Stepanyants acknowledges the funding of this study provided by the RF Council on Grants for the state support of Leading Scientific Schools of the Russian Federation (Grant No. NSH-70.2022.1.5).

## AUTHOR DECLARATIONS

### Conflict of Interest

The authors have no conflicts to disclose.

### Author Contributions

**Zhao Zhang:** Formal analysis (equal); Investigation (equal); Validation (equal); Visualization (equal); Writing – original draft (equal). **Wencheng Hu:** Formal analysis (equal); Investigation (equal); Software (equal); Validation (equal); Visualization (equal). **Qi Guo:** Project administration (equal); Supervision (equal); Validation (equal). **Yury Stepanyants:** Conceptualization (equal); Formal analysis (equal); Investigation (equal); Methodology (equal); Project administration (equal); Supervision (equal); Validation (equal); Writing – original draft (equal); Writing – review & editing (equal).

## DATA AVAILABILITY

The data that support the findings of this study are available from the corresponding author upon reasonable request.

## REFERENCES

[1]W. Hu, Z. Zhang, Q. Guo, and Y. Stepanyants, "Solitons and lumps in the cylindrical Kadomtsev–Petviashvili equation. I. Axisymmetric solitons and their stability," Chaos (accepted).
[2]R. S. Johnson, "Water waves and Korteweg–de Vries equations," J. Fluid Mech. **97**(4), 701–719 (1980).
[3]C. Klein, V. B. Matveev, and A. O. Smirnov, "Cylindrical Kadomtsev–Petviashvili equation: Old and new results," Theor. Math. Phys. **152**(2), 1132–1145 (2007).
[4]B. B. Kadomtsev and V. I. Petviashvili, "On the stability of solitary waves in weakly dispersing media," Sov. Phys. Dokl. **15**, 539–541 (1970).
[5]V. E. Zakharov, "Turbulence in integrable systems," Stud. Appl. Math. **122**, 219–234 (2009).
[6]D. E. Pelinovsky and Y. A. Stepanyants, "Self-focusing instability of plane solitons and chains of two-dimensional solitons in positive-dispersion media," JETP **77**(4), 602–608 (1993).
[7]V. B. Matveev and M. A. Salle, *Darboux Transformations and Solitons* (Springer-Verlag, 1991).
[8]V. S. Dryuma, "On the integration of the cylindrical Kadomtsev–Petviashvili equation by the method of the inverse problem of scattering theory," Sov. Math. Dokl. **27**, 6–8 (1983).
[9]V. E. Zakharov and A. B. Shabat, "A scheme for integrating the non-linear equations of mathematical physics by the method of the inverse scattering problem. I," Func. Anal. Appl. **8**, 226–235 (1974).
[10]C. Lester, A. Gelash, D. Zakharov, and V. E. Zakharov, "Lump chains in the KP-I equation," Stud. Appl. Math. **147**(4), 1425–1442 (2021).
[11]Y. A. Stepanyants, D. V. Zakharov, and V. E. Zakharov, "Lump interactions with plane solitons," Radiophys. Quant. Electron. **64**, 665–680 (2022).
[12]K. A. Gorshkov, D. E. Pelinovsky, and Y. A. Stepanyants, "Normal and anomalous scattering, formation and decay of bound states of two-dimensional solitons described by the Kadomtsev–Petviashvili equation," JETP **104**, 2704–2720 (1993).
[13]Z. Zhang, B. Li, J. Chen, Q. Guo, and Y. Stepanyants, "Degenerate lump interactions within the Kadomtsev–Petviashvili equation," Commun. Nonlinear Sci. Numer. Simul. **112**, 106555 (2022).
[14]Z. Zhang, Q. Guo, and Y. Stepanyants, "Creation of weakly interacting lumps by degeneration of lump chains in the KP1 equation," Chaos, Solitons Fractals **170**, 113398 (2023).
[15]J. G. Rao, J. S. He, and B. A. Malomed, "Resonant collisions between lumps and periodic solitons in the Kadomtsev– Petviashvili I equation," J. Math. Phys. **63**, 013510 (2022).
[16]Z. Zhang, B. Li, J. Chen, Q. Guo, and Y. Stepanyants, "Peculiarities of resonant interactions of lump chains within the KP1 equation," Phys. Scr. **97**, 115205 (2022).
[17]F. Calogero and A. Degasperis, "Solution by the spectral-transform method of a nonlinear evolution equation including as a special case the cylindrical KdV equation," Lett. Nuovo Cim. **23**, 150–154 (1978).
[18]F. Calogero and A. Degasperis, *Spectral Transform and Solitons: Tools to Solve and Investigate Nonlinear Evolution Equations* (North-Holland Publishing Co., Amsterdam, Holland, 1982).
[19]A. Nakamura and H.-H. Chen, "Soliton solutions of the cylindrical KdV equation," J. Phys. Soc. Jpn. **50**, 711–718 (1981).
[20]R. S. Johnson, "On the inverse scattering transform, the cylindrical Korteweg–de Vries equations and similarity solutions," Phys. Lett. A **72**, 197–199 (1979).
[21]D. E. Pelinovsky and Y. A. Stepanyants, "New multisoliton solutions of the Kadomtsev–Petviashvili equation," JETP Lett. **57**(1), 24–28 (1993).
[22]W. Hu, W. Huang, Z. Lu, and Y. Stepanyants, "Interaction of multi-lumps within the Kadomtsev–Petviashvily equation," Wave Motion **77**, 243–256 (2018).
[23]N. Singh and Y. Stepanyants, "Obliquely propagating skew KP lumps," Wave Motion **64**, 92–102 (2016).
[24]Z. Zhang, X. Yang, B. Li, Q. Guo, and Y. Stepanyants, "Multi-lump formations from lump chains and plane solitons in the KP1 equation," Nonlinear Dyn. **111**, 1625–1642 (2023).
[25]N. Hershkowitz and T. Romesser, "Observations of ion-acoustic cylindrical solitons," Phys. Rev. Lett. **32**(11), 581–583 (1974).
[26]S. Maxon and J. Viecelli, "Cylindrical solitons," Phys. Fluids **17**(8), 1614–1616 (1974).
[27]L. A. Ostrovskii and V. I. Shrira, "Instability and self-refraction of solitons," Sov. Phys. JETP **44**(4), 738–742 (1976).